Proceedings of 2012 IEEE
International Conference on Mechatronics and Automation
August 5 - 8, Chengdu, China

Robust Weld Line Detection with Cross Structured Light and Hidden Markov Model

Liguo Zhang, Jianbin Jiao, Qixiang Ye, Zhenjun Han, Wei Yang
Graduate University of Chinese Academy of Sciences, Beijing, China
jiaojb@ gucas.ac.cn

***Abstract* - In this paper, we propose a vision-based weld line detection system with cross structured light (CSL) and Hidden Markov Model (HMM). Our consideration is that the laser stripes projected by CSL can reflect the convex shapes of weld lines, capture horizontal and vertical weld lines simultaneously and are insensitive to illumination changes. The Hidden Markov Model filters out various noises on the weldment surface and then detects laser stripes precisely, which guarantees the accuracy of weld line location. Experiments on practical and simulated datasets show that the results of our approach have great improvement to classical Hough transform based method.**

Index Terms* -*Weld line detection, Cross structured light, HMM

I. INTRODUCTION

Automatic weld inspection systems are required to guarantee the safety of various kinds of metal weldment facilities, such as towers in wind power equipments, storage tanks, and metal pipelines [1]. Weld line detection in a moving platform (such as a wall climbing robot) is the primal problem to be investigated in these systems. In general, the weld lines have same colour with their background (metal weldment facilities). Many facilities are located in outdoor conditions and then weld lines on them are dirty with dust, oil, rust or bird droppings. In addition, the illumination on the weld lines is often either strong or weak for the reason of sunshine. These factors make the precise weld line detection a very challenging problem.

In recent years, vision sensing and computer vision techniques are attracting considerable attention in weld line detection. In [2][3], Li et al designed a vision measurement and defect detection system of the weld bead based on structured light. The system uses intensity distribution and continuity constraints to extract the stripe in an image, uses the second derivative of the stripe to extract feature points of the weld line, and finally takes the smallest intensity of the corresponding pixels in a sequence of images for tracking. In [4], Yang et al designed an automatic weld seam tracking system based on structured light for gas metal arc welding. The system employs Hough transform to extract laser stripes and a Neural Network based on the generalized delta rule algorithm is used to control welding process. In [5], Liu et al designed a robot real-time seam tracking system based on laser vision, and used an improved image filtering to recognize and extract seam images. In [6], Wu et al proposed a novel seam measuring method to accurately acquire seam gap width and seam surface normal vector. The above mentioned systems are mainly used for welding process instead of weld line inspection. The main problem is to detect and track seam gap for welding, considering little about illumination and noises in outdoor scenes.

On the other hand, weld line detection for inspection is also investigated. In [7], Carvalho et al used distance sensors to identify weld lines of Spherical Tanks. Molina et al [8][9] segmented the image of weld line based on texture to a binary image, and used a modified Hough transform to detect the position and orientation of weld line on storage tank. Finally, they used a fault-tolerant estimation process based on an α-β filter to improve the robustness of system. Despite of their advantages, these systems do not use CSL and therefore it is difficult for them to detect intersections of weld lines. In [10], Strobl et al presented a robust stripe segmentation algorithm for 3D modeling. They detected stripe edge, color and width by means of Look-Up Table, which may be affected by noises.

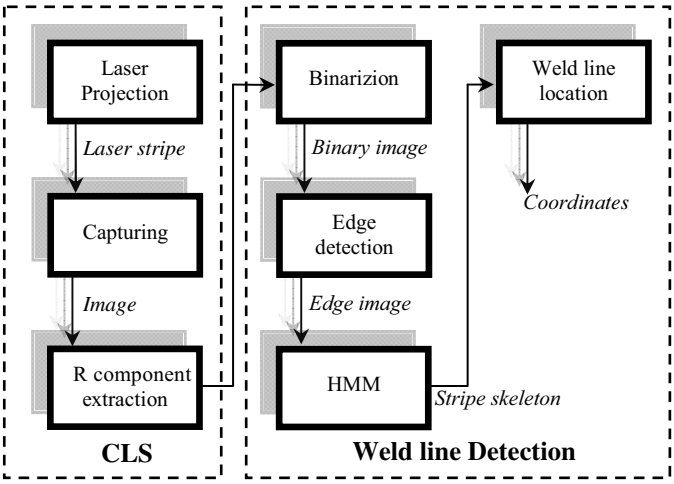

Fig. 1 Flowchart of the proposed CSL based weld line detection approach.

In this paper we present a computer vision sensing system based on a CSL and HMM for outdoor weld line inspection. The follow chart of the proposed system is shown as Fig.1. In the system, a CSL platform is designed to project a red cross laser stripe on the weldment surface, which is then captured into an image with a CCD camera. Then an edge map is calculated from the binaralized red color component of the image. An HMM is then applied on the edge map to detect laser stripes. Finally, we define a measurement to search and locate weld lines. The laser stripes projected by CSL can reflect height of weld lines with respect to the weldment surface, capture horizontal and vertical weld lines simultaneously and are insensitive to illumination changes.

The Hidden Markov Model filters out various noises when detecting laser stripes, which guarantees the accuracy of weld line location.

The remainder of this paper is organized as follows: The CSL platform design is presented in section II. Weld line detection approach is presented in Section III. We present experiments in Section IV and conclude the paper in Section V.

II. CROSS STRUCTURED LIGHT (CSL) PLATFORM DESIGN

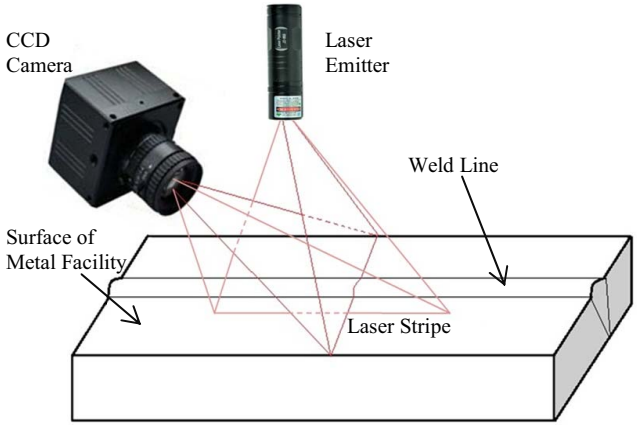

(a)

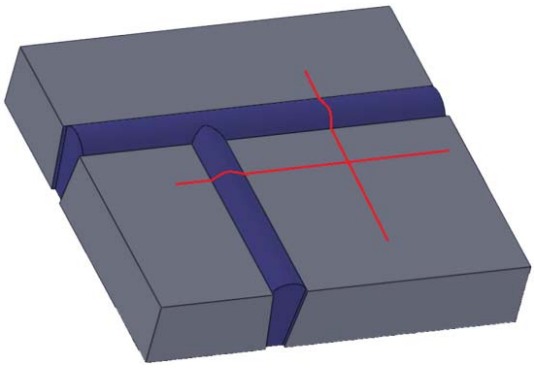

(b)

Fig.2 (a) Illustration of CSL platform. (b) illustration of laser stripes on a weldment surface of a cross weld line.

A CCD camera together with a laser emitter is used to design the CSL platform. The laser emitter is fixed to perpendicular to the weldment surface. The CCD camera is fixed with a 45 degree angle to the weldment surface. In general, weld line have convex shapes and are higher than facility surface, consequently, there are convex arcs ("Ω" shapes) appear on the strips around the weld lines, as showed in Fig.2a. When the platform is close to the intersection of vertical and horizontal weld lines, two convex arcs will appear on the strips, as showed in Fig.2b. These characteristics of the designed CSL platform enable it detect single or cross weld lines.

When performing weld line detection, the platform will move along the weld line on a wall climbing robot. It capture 20 images per second to detect weld lines. Detected results in image space will be converted into the Cartesian space of robot end-effecter frame [11,12] and then is used to control the movement of the robot. But the robot controller is out of the scope of this paper.

III. WELD LINE DETECTION

It can be seen in Fig.3 that when the stripe meets the weld line, it appears like a convex arc because of the height of weld line. It must be mentioned that in practical conditions, the heights of weld lines are often very small, consequently, it is difficult to discriminate the convex arcs from the stripe lines. Therefore, the most important thing in our approach is to locate the laser stripes precisely.

A red component image is firstly extracted from the captured image. A threshold determined with histogram analysis method is used to convert the red component image into a binary image. Then, Canny edge image of the binarized image is extracted with Canny operator [13], as shown in Fig.3b.

In outdoor conditions, the weldment surfaces are often dirty for the cover of dust, oil, rust, bird droppings. The reflection of natural light may also bring noises. It can be seen on Canny image that there are some noise edge pixels which will affect the locating of laser stripes. Therefore, we employ an HMM to filter out noises on laser stripes and locate weld lines precisely. Here, HMM is used as a global optimization model. Given the observation sequence, we choose a state sequence which is optimal in terms of the smoothness and linearity of laser stripes.

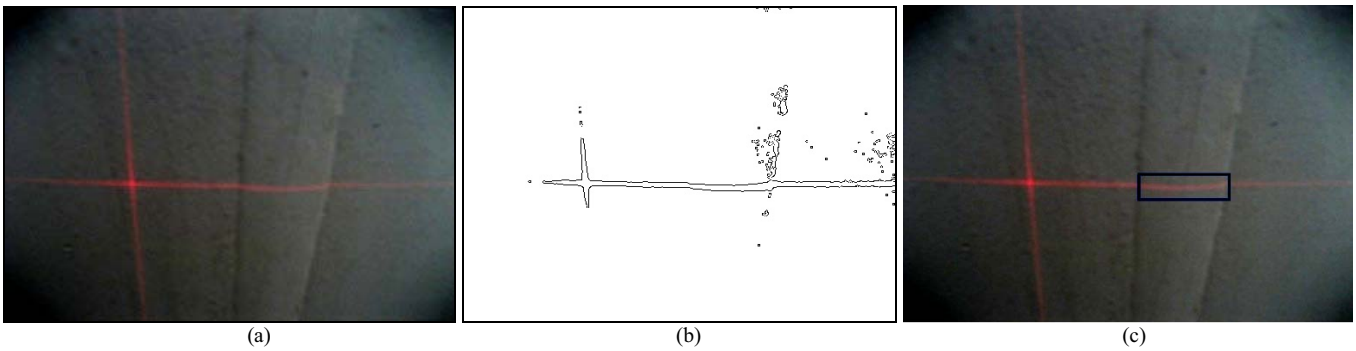

(a) (b) (c)

Fig.3 Extraction of edge image and filtering the stripe edges with an HMM. (a) A captured laser stripe image, (b) Canny edge image, (c) A weld line location on laser stripe

A. Laser Stripe Detection with HMM

The detection of a laser stripe in an edge image is defined as a decoding process of HMM [14,15]. A stripe is described with a state $\omega_r(t)$ at time step t. The state count of a horizontal stripe is equal to the image width and that of a vertical stripe is equal to the image height. The state can only be observed through a sequence of observed variables $V=\{v(1),...,v(T)\}$. Given the observation sequence V, the problem is to choose a state sequence $\omega=\{\omega_r(0),...,\omega_r(T)\}$ which is optimal in terms of defined observation and transition probability, which is described as

$$P(V)=\prod_{t=1}^{T}\sum_{r=0}^{R(t)}P\big(v(t)\,|\,\omega(t)\big)P\big(\omega(t)\,|\,\omega(t-1)\big), \tag{1}$$

where r denotes he index of hidden states in each step. $R(t)$ denotes the amount of the hidden states of step t and T denotes the sequence length.

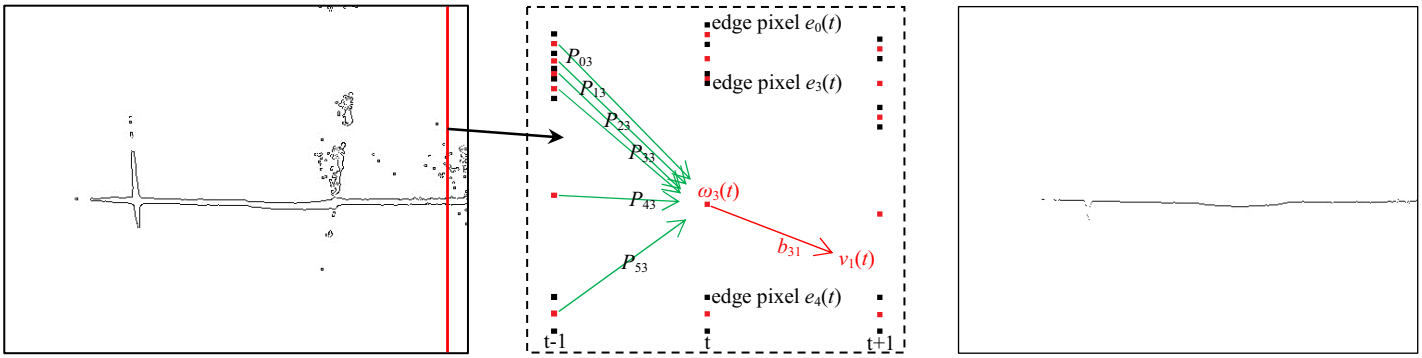

Fig.4 HMM for stripe detection. (a) Edge image, and (b) illustration of steps of HMM, the states are from three columns of edge pixels of (a), where black points represent edge pixels, and red points represent midpoints of adjacent edge pairs.(c) Detected stripe skeleton.

It can be seen in Fig.3b that there are two parallel skeletons for a horizontal stripe. Consequently the edge pixels on the stripe form a sequence of edge pairs with relative fixed distance intervals. The isolated edge pixels out of the parallel skeletons are often noises. Let $e_r(t), t=1,...,T, r=0,...,R(t)$ denote the coordinates of a column of edge pixels at step t. The midpoint of $e_r(t)$ and $e_{r+1}(t)$ is defined as a state $\omega_r(t)$. $R(t)$ denotes the amount of mid-points at step t. $L_r(t)=|e_r(t)-e_{r+1}(t)|, t=1,...,T$ denotes a distance between edge pixel $e_r(t)$ and $e_{r+1}(t)$, which is defined as the observation value. $m_r(t), t=1,...,T$ denotes the color mean of the pixels between the two adjacent edge pixels $e_r(t)$ and $e_{r+1}(t)$, which is used to calculated transition probability. For example, in Fig.4b, $m_3(t)$ is mean value of pixels between $e_3(t)$ and $e_4(t)$ of adjacent edge pixels. If there is no any edge point in a column, the model will skip this column.

Given the above definitions, we can build the HMM for a stripe. The initial state probability is set as $P(\omega(0))=\frac{1}{T}$. The observed probability is defined as

$$P\big(v(t)\,|\,\omega(t)\big)=\begin{cases}1.0, & if\ \big(L_r(t)\big)<T_e\\ 0.0, & \end{cases}, \tag{2}$$

where T_e is a empirically determined threshold, which is set to 20 pixels when image pixels are 500×400. By (2) we know that if the distance between a two adjacent edge pixels is lager that T_e, the observation probability will be zero, which is used to constrain the width of the stripe. The transition probability is calculated by

$$P\big(\omega_j(t)\,|\,\omega_i(t-1)\big)=\exp\left\{-\big(w_1,w_2\big)\cdot\left(\frac{d_{ij}^{\,2}}{\sigma_d^2},\frac{f_{ij}^{\,2}}{\sigma_f^2}\right)^{t}\right\}, \tag{3}$$

where d_{ij} denotes the distance between two midpoints of two adjacent time steps. For example, the distance from midpoint i of time step $t-1$ to midpoint j of time step t is $d_{ij}=\sqrt{(e_i(t-1)-e_j(t))^2+(e_i(t-1)-e_j(t))^2}$. $e_i(t-1)$ and $e_j(t)$ are coordinates of midpoint i at time step $t-1$ and midpoint j at time step t, respectively. f_{ij} denotes the difference between the means of red color component of two adjacent steps. $f_{ij}=|m_i(t-1)-m_j(t)|$ is defined as the spatial distance between $m_i(t\text{-}1)$ of step t 1 and $m_j(t)$ of step t. σ_d^2 is the variance of distance , which is calculated with

$$\sigma_d^2=\frac{\sum_{t=0}^{T}\sum_{r=0}^{R(t)}\big[d_{ij}-\bar{d}\big]^2}{\prod_{t=0}^{T}R(t)}, \tag{4}$$

where $\bar{d}$ is the mean of all d_{ij}. σ_f^2 is the variance of color difference, which is calculated with

$$\sigma_f^2=\frac{\sum_{t=0}^{T}\sum_{r=0}^{R(t)}\big[f_{ij}-\bar{f}\big]^2}{\prod_{t=0}^{T}R(t)}, \tag{5}$$

where $\bar{f}$ is the mean of all f_{ij}. w_1, w_2 are two weights to balance the importance of distance and color, and w_1+w_2=1.0.

The problem of laser stripe detection is solved by maximizing the value of (1), which is regarded as a path optimization problem. On the optimized path, the transition cost is minimized in terms of a reasonable observation probability. The problem is solved by using a Viterbi recoding algorithm[16] and a image of filtered edge pixels can be obtained as a clear skeleton of laser stripe, as shown in Fig.5a.

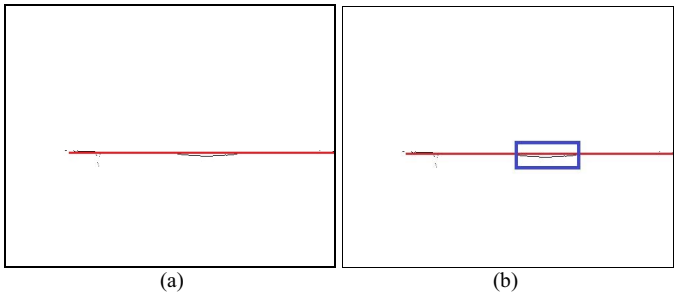

(a) (b)

Fig.5 (a)Base line of stripe skeleton, (b)Weld line convex arc location.

B. Weld Line Location

From Fig.4c we can see the laser stripe appears like a convex arc on a weld line. Therefore the weld line can be located by detecting the convex arc. We first use Hough transform to detect a line as base line, as shown in Fig.5a. Then we define a function to detect convex arc by the following equation:

$$F = \max_{W,n} \frac{1}{W \times \sigma^2} \left(S \times \sum_{t=n}^{W+n} C\left(\omega(t) \mid \omega(t-1)\right) \right), \qquad (6)$$

where W denotes the width of the instantaneous slide window. n represents the first point (step) of the slide window. S is the area of the closed region between the convex arc and the base line. (equal to the number of pixels in the region). C=1/P is the transition cost in the slide window, which is defined as the reciprocal of transition probability of (3). σ^2 is the variance of values of the distance from the points on convex arc to the base line in the window.

When performing detection, we define two constraints: *i*) the region between the convex arc and the base line must be closed; *ii*) the area S must be larger than a empirically predefined threshold H (H=200 when image pixels are 500×400). This can eliminate some jump points from detected area. Given the value of W, we search from the start pixel of the filtered stripe line to find a position that maximized the value of (6). By sliding window and searching procedure, the location of the convex arc (weld line position) is determined. When the value of W cannot be determined empirically, we use a searching algorithm to change its value to maximize (6) and finally determine the both size and the position of the arc.

In addition, the system can detect convex arc in the vertical laser stripe (Eq. (6)). Considering the noise or long-time absence of the weld line in the vertical direction, the constrain *ii* above can effectively filter out some invalid detection results.

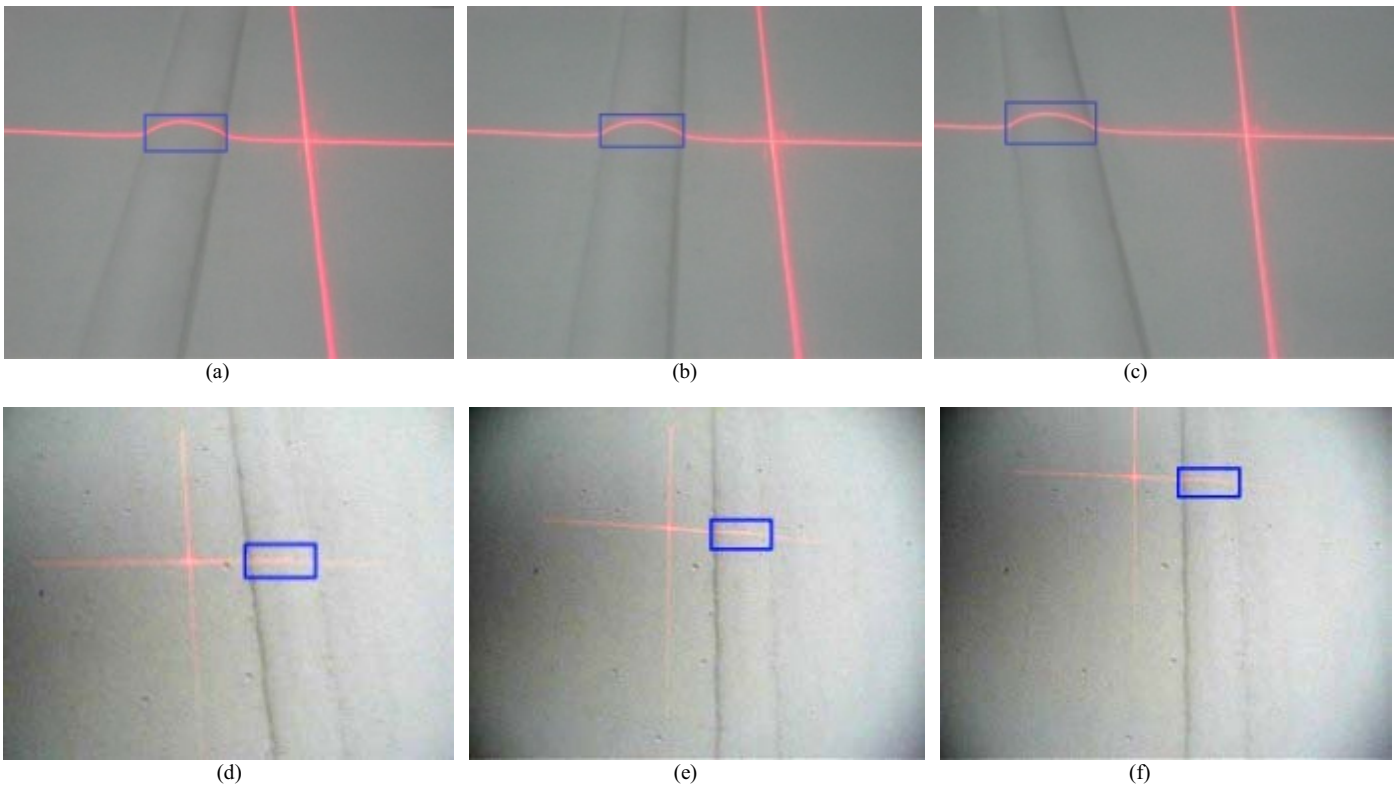

(a) (b) (c)

(d) (e) (f)

Fig.6 Detection results of indoor and outdoor data.

IV. EXPERIMENTS

The proposed approach has been tested on several video sequences. Fig.6a, Fig.6b and Fig.6c are the detection results from simulated indoor data. Fig.6d, Fig.6e and Fig.6f show detection results of weld lines on a wind power tower when there were high illumination. It can be seen that our proposed approach can detect the weld line very well, showing its robustness to illumination.

The proposed approach is quantitively evaluated by comparing the detection results with manually marked weld line ground-truth in 100 frames(images size are all set as 500×400). Two end points A and B on the weld line, as shown in Fig.7a, are used as feature points to measure the detection errors. The errors of our proposed approach are compared with those of Hough Transform method. It can be seen in Fig.7b and Fig.7c that errors of our proposed approach are much lower than those of Hough transform, showing that it is more robust when performing detection.

As shown in Table 1, the average error of our approach in image space is five pixels smaller than that of Hough transform method. In the Cartesian space of the end-effectors the average error of our approach is 3mm smaller than that of Hough transform method. The improvement is very significant.

When the platform moves close to the intersection of horizontal vertical weld lines, two laser stripes are detected a weld line, as shown in Fig.8(next page). As the platform moves onto intersection point, there is only one weld line detected in the vertical orientation. In this condition, the system can identify a weld line intersection, and then it can delivery inductor to the robot to make a turn. In Fig.8, we use a visualized a detected weld line in successive video frames, which shows the stability of our approach.

TABLE I
COMPARISONS OF ERRORS OF DETECTED WELD LINE FEATURE POINTS(MIDPOINT OF A AND B) MID-POINTS

Methods	Maximum error (pixels)	Minimum error (pixels)	Average error (pixels)
Our approach	30	0	5
Hough transform	60	5	35

Methods	Maximum error of end-effecter (mm)	Minimum error of end-effecter (mm)	Average error of end-effecter (mm)
Our approach	12	0	3
Hough transform	23	3	14

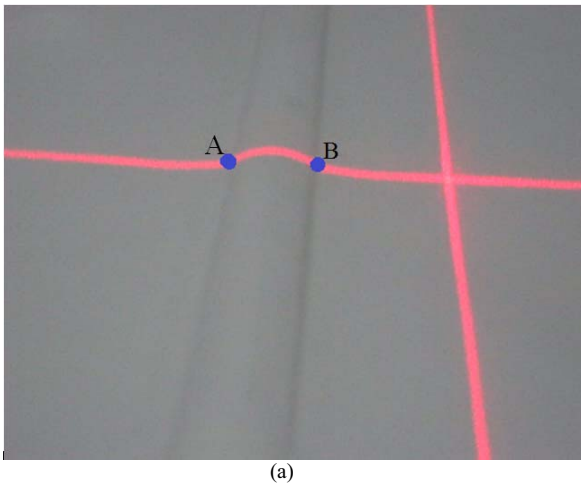

(a)

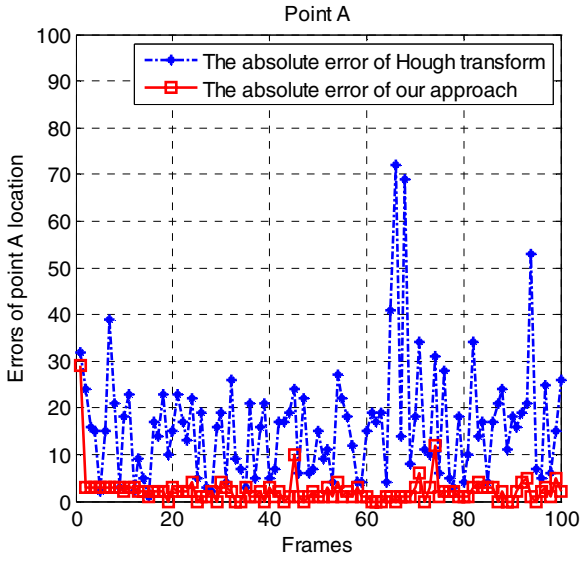

(b)

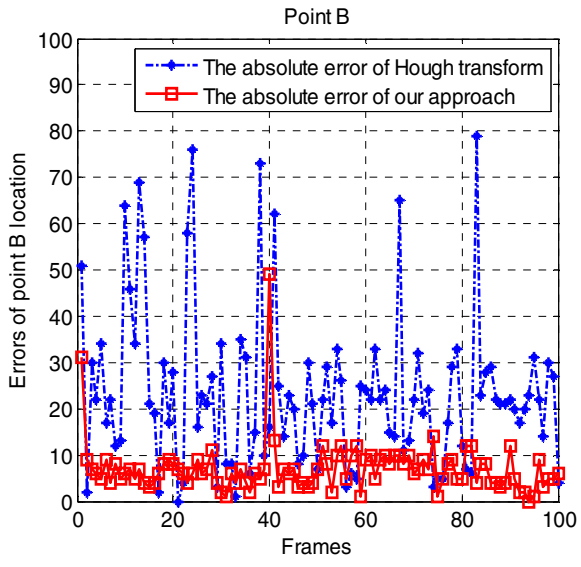

(c)

Fig.7 Evaluation and comparison of the proposed approach. (a) illustrates the feature points for error evaluation, (b) is the error of point A and (c) of point B.

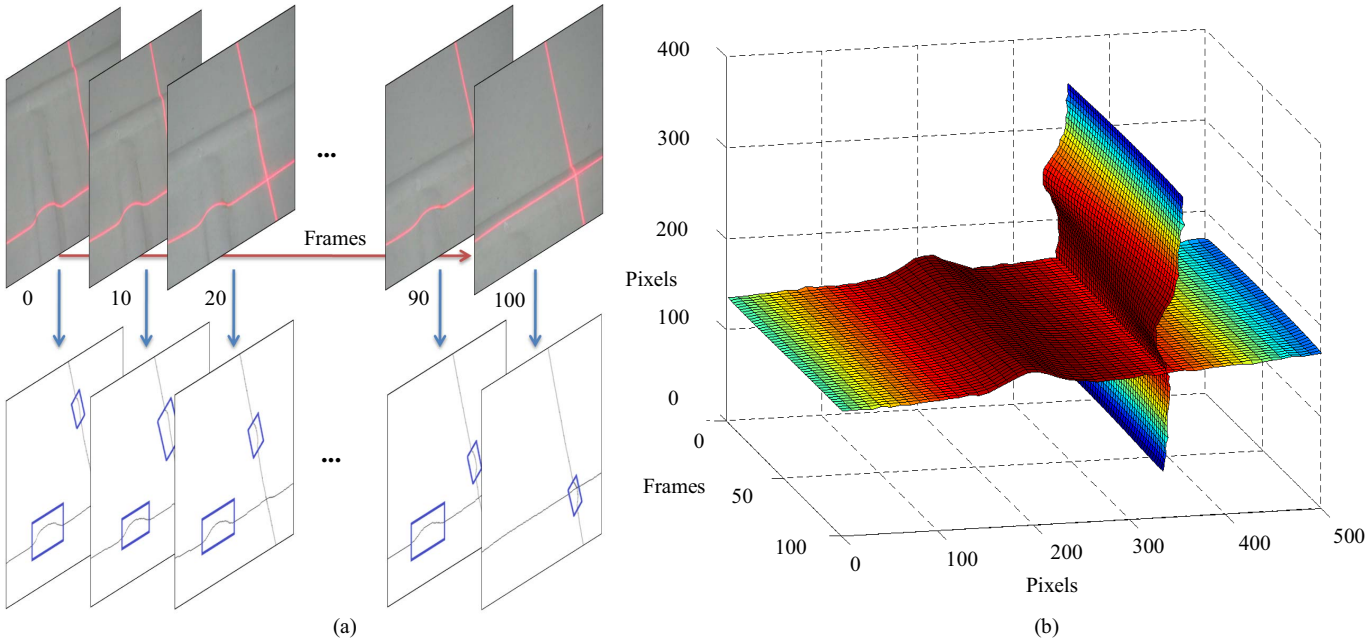

(a) (b)

Fig.8. (a) From left to right, images are captured when the platform is moving close to a weld line intersection. (b) shows the weld locations in successive video frames

V. CONCLUSIONS

In the paper, we proposed a vision based weld line detects approach with a CSL platform and a HMM. The proper observation and transition probability for the HMM are defined when detecting laser stripes. A searching procedure with defined Straight Measurement is used to locate weld line in edge map of laser stripes. We validate the effectiveness of the proposed approach when detecting single and cross weld lines in even noisy background. The main reason for the errors is uneven of weld line or defect of weldment surface. In the future, temporal filtering in image sequences, such as tracking algorithms, will be considered to further improve the robustness of the system.

ACKNOWLEDGEMENT

This work is supported in part by National Basic Research Program of China (973 Program) with Nos. 2011CB706900, 2010CB731800, and National Science Foundation of China with No. 61039003.

REFERENCES

[1] W. A. K. Deutsch, P. Schulte, M. Joswig and R. Kattwinkel, "Automatic inspection of welded pipes with ultrasound," *Proceedings of the 9th ECNDT*, pp.1-14, September 2006.

[2] Y. Li, Y.F. Li, Q.L. Wang, D. Xu, M. Tan, "Measurement and defect detection of the weld bead based on online vision inspection". *IEEE Transactions on Instrumentation and Measurement*, vol. 5, no.9, 2010, pp. 1841–1849

[3] Y. Li, Q.L. Wang, Y.F. Li; D. Xu, Min Tan, "On-line visual measurement and inspection of weld bead using structured light", *IEEE Instrumentation and Measurement Technology Conference Proceedings*, pp. 2038 – 2043, May 2008.

[4] Sang-Min Yang, Man-Ho Cho, Ho-Young Lee and Taik-Dong Cho, "Weld line detection and process control for welding automation" *Measurement Science and Technology*, vol.18, no.3, pp. 819–826 , 2007.

[5] Liu Suyi, Liu Lingteng, Zhang Hua, Bai Jianjun, Wang Guorong, "Study of robot seam tracking system with laser vision" *IEEE International Conference on Mechatronics and Automation*, pp.1296 – 1301, August 2009.

[6] Jiayong Wu; Pingjiang Wang; Xingdou Fu; Biao Liu; Jihong Chen, "A novel seam measuring method of complex tight butt joint for laser welding",*IEEE International Conference on Mechatronics and Automation*, pp. 2548 – 2553, August 2009.

[7] Carvalho, E.,Luciano, B.A,Freire, R,Molina, L,Freire, E.O, "Fault-tolerant weld line detection for automatic inspection of storage tanks based on distance and visual information fusion". *IEEE Instrumentation and Measurement Technology Conference*, pp.791 – 796, May 2009.

[8] Molina, L,Carvalho, E. A. N, Freire, E. O, Montalvão-Filho, J. R, Chagas, F. de A. "A robotic vision system using a modified Hough transform to perform weld line detection on storage tanks", *IEEE Latin American Robotic Symposium – LARS.* pp.45-50, 2008.

[9]Lucas Molina, Eduardo O. Freire, Elyson A. N. Carvalho, Joao Carlos Basilio, "Fault-tolerant weld line detection for automatic inspection of storage tanks based on visual information fusion and *a-β* filter". *Instrumentation and Measurement Technology Conference*, *Robotics Symposium and Intelligent Robotic Meeting,* pp.25 – 29, *October 2010*

[10] Strobl, K, Sepp, W, Wahl, E, Bodenmüller, T, Suppa, M, Seara, J, Hirzinger, G, "The DLR multisensory hand-guided device: the laser stripe profiler", *IEEE International Conference on Robotics and Automation, 2004. Proceedings,* pp. 1927-1932, May 2004

[11] D. Xu, L. Wang, Z. Tu, and M. Tan, "Hybrid visual servoing control for robotic arc welding based on structured light vision," *Acta Automatica Sinica*, vol. 31, no. 4, pp. 596–605, 2005.

[12] D. Xu, Z. Tu and M. Tan. "Study on visual positioning based on homography for indoor mobile robot". *Acta Automatica Sinica*, vol. 31, no. 3, pp. 464–469, 2005.

[13] J. Canny, "A computational approach to edge detection," *IEEE Transactions on Pattern Analysis Machine and Intelligence*, vol. 8, pp. 679-698, 1986.

[14] Rabiner. L, Juang. B, "An introduction to hidden Markov models", *IEEE ASSP Magazine,* Vol.3, pp.4-16, Jan 1986

[15] Richard O.Duda, Peter E.Hart, David G.Stork. "Pattern Classification, Second Edition". *John Wiley & sons, Inc.*, pp.128-137, 2001.

[16] H.L. Lou. "Implementing the Viterbi algorithm". *IEEE Signal Processing Magazine*, vol.12, no.5, pp.42-52, September 1995.